

Article

Teladorsagia circumcincta 1,6-Bisphosphate Aldolase: Molecular and Biochemical Characterisation, Structure Analysis and Recognition by Immune Hosts

Saleh Umair ^{1,*}, Charlotte Bouchet ¹, Nikola Palevich ¹ and Heather Simpson ²

¹ AgResearch Ltd., Hopkirk Research Institute, Grasslands Research Centre, Tennent Drive, Private Bag 11008, Palmerston North 4442, New Zealand; charlotte.bouchet@agresearch.co.nz (C.B.); nik.palevich@agresearch.co.nz (N.P.)

² School of Veterinary Sciences, Massey University, Private Bag 11222, Palmerston North 4440, New Zealand; H.V.Simpson@massey.ac.nz

* Correspondence: saleh.umair@agresearch.co.nz

Abstract: A 1095 bp full length cDNA encoding *Teladorsagia circumcincta* aldolase (*Tci*ALDO-1) was cloned and expressed in *Escherichia coli*. Recombinant *Tci*ALDO-1 was purified, and its kinetic properties determined. The predicted protein consisted of 365 amino acids, and was present as a single band of about 44 kDa on SDS-PAGE. Multiple alignments of the protein sequence of *Tci*ALDO-1 with homologues from other helminths showed the greatest similarity (93%) to the aldolases of *Haemonchus contortus* and *Dictyocaulus viviparus*, 82–86% similarity to the other nematode sequences, and 68–71% similarity to cestode and trematode enzymes. Substrate binding sites and conserved regions were identified, and were completely conserved in other homologues. At 30 °C, the optimum pH for *Tci*ALDO-1 activity was pH 7.5, the V_{\max} was $432 \pm 23 \text{ nmol} \times \text{min}^{-1} \times \text{mg}^{-1}$ protein, and the apparent K_m for the substrate fructose 1,6-bisphosphate was $0.24 \pm 0.01 \text{ } \mu\text{M}$ (mean \pm SEM, $n = 3$). Recombinant *Tci*ALDO-1 was recognized by antibodies in both serum and saliva from field-immune sheep in ELISA, however, that was not the case with nematode-naïve sheep. *Teladorsagia circumcincta* fructose 1,6-bisphosphate aldolase appears to have potential as a vaccine candidate to control this common sheep parasite.

Keywords: aldolase; cloning; expression; kinetic properties; *Teladorsagia circumcincta*



Citation: Umair, S.; Bouchet, C.; Palevich, N.; Simpson, H. *Teladorsagia circumcincta* 1,6-Bisphosphate Aldolase: Molecular and Biochemical Characterisation, Structure Analysis and Recognition by Immune Hosts. *Parasitologia* **2021**, *1*, 1–11. <https://doi.org/10.3390/parasitologia1010001>

Received: 9 December 2020

Accepted: 12 January 2021

Published: 30 January 2021

Publisher's Note: MDPI stays neutral with regard to jurisdictional claims in published maps and institutional affiliations.



Copyright: © 2021 by the authors. Licensee MDPI, Basel, Switzerland. This article is an open access article distributed under the terms and conditions of the Creative Commons Attribution (CC BY) license (<https://creativecommons.org/licenses/by/4.0/>).

1. Introduction

Fructose 1,6-bisphosphate aldolase (FBA) (EC 4.1.2.13) catalyses the reversible reaction that splits fructose 1,6-bisphosphate into the 3-phosphate dihydroxyacetone phosphate (DHAP) and glyceraldehyde 3-phosphate (G3P). The forward reaction occurs during glycolysis and the reverse reaction forms fructose 1,6-bisphosphate during gluconeogenesis. FBA enzymes belong to two classes depending on the mechanism of the reaction: class I, which form covalent Schiff-base conjugates with a conserved lysine, are present mainly in higher eukaryotes and a few bacteria, whereas class II require a divalent metal ion as cofactor for enzymatic activity and are found principally in bacteria, algae and fungi [1–4]. Thus, class I and II enzymes can be distinguished by inhibition of the latter by ethylene diamine tetraacetic acid (EDTA). There are three isoforms of vertebrate FBA: aldolase A which is principally expressed in muscle, aldolase B in liver and aldolase C in brain.

The genes encoding FBAs have been sequenced from the free-living nematode *Caenorhabditis elegans* [5], the animal-parasitic *Haemonchus contortus* [6], the plant-parasitic *Heterodera glycines* and *Globodera rostochiensis* [7], as well as helminths, including *Schistosoma mansoni* [8] *Echinococcus granulosus* [9], *Clonorchis sinensis* [10], *Schistosoma japonicum* [11] and *Opisthorchis viverrini* [12]. As nematode FBAs were shown to have some structural properties similar to vertebrate FBAA, but catalytic properties more like those of FBAC, aldolases

were suggested to be the products of primordial genes from which vertebrate FBA genes have evolved [13]. Subsequent genetic studies have shown that in *C. elegans* there are two isozymes encoded by different genes, one of which has similar kinetic properties to vertebrate aldolase C and the other broader substrate specificity in addition to fructose 1,6 bisphosphate [5], which could explain the earlier conclusions about nematode aldolases.

The kinetic properties of FBA enzymes are generally typical of aldolases, such as the typical temperature and pH optima of 40 °C and pH 7.5 respectively of the *H. contortus* enzyme [6]. The reported K_m of purified nematode aldolases varied between species and even within studies, e.g. the aldolase in homogenates of *H. glycines* had a lower activity than either the *C. elegans* or *Panagrellus redivivus* enzymes [14]. Enzyme activity declined with age in the free-living *Turbatrix aceti* [15]. Parasitic helminths may have more active enzymes than their hosts, as seen for *S. japonicum* FBA, which had a lower apparent K_m of 0.06 μ M and higher activity than that of human FBAA [11].

Aldolase, like many other glycolytic enzymes, has both intra- and extra-cellular moonlighting activities in parasites in addition to its enzymatic function [16]; these include plasminogen binding [17] and immunomodulation [18]. It is released into the extracellular environment and can be detected in excretory/secretory (ES) products [17,19,20] and has been also located in the tegument of adult *Schistosoma bovis* [17] and *S. mansoni* [8].

In the present study, the cDNA encoding *T. circumcincta* aldolase (*Tci*ALDO-1) was cloned, expressed in *Escherichia coli*, the recombinant protein was purified and some kinetic properties determined. Enzyme-linked immunosorbent assays (ELISAs) were performed to determine if the enzymes were recognised by saliva and serum from sheep previously exposed to nematode parasites in the field.

2. Material and Methods

All chemicals used in these experiments were purchased from the Sigma Chemical Co. (St. Louis, MO, USA) unless stated. Use of lambs for parasite culturing and harvesting adult worms for molecular biology studies was approved in protocol #13502 by the AgResearch Grasslands Animal Ethics Committee (protocol #13052).

2.1. Parasite Culture and Collection

Pure cultures of *T. circumcincta* were obtained by passaging larvae through sheep. Adult worms were recovered from the abomasa of infected sheep, as described previously [21]. Briefly, abomasal contents were mixed with agar, and the solidified agar blocks incubated at 37 °C in a saline bath. Clumps of parasites were collected and frozen at –80 °C for RNA collection.

2.2. RNA Isolation and cDNA Synthesis

RNA was isolated from adult worms as described previously [22]. Briefly, about 50–100 μ L packed volume of adult *T. circumcincta* were ground to powder using in 1 mL Trizol (Life Technologies, Carlsbad, CA, USA) under liquid N₂. The quality of the isolated RNA was assessed by running in 1% TAE gel and concentration using Nanodrop (ThermoFisher Scientific, Waltham, MA, USA). First strand cDNA was synthesized from 1 μ g total RNA using a iScript Select cDNA Synthesis Kit (Bio-Rad, Auckland, New Zealand) as per the manufacturer instructions.

2.3. Cloning and Expression of *T. circumcincta* Recombinant *Tci*ALDO-1 in *E. coli*

A partial *T. circumcincta* ALDO sequence TDC00486 (NEMBASE) containing the 5' end was used, and the 3' of *Tci*ALDO-1 cDNA was obtained by 3' Rapid amplification of cDNA Ends (RACE) using *T. circumcincta* adult RNA, as outlined by the manufacturer. The full length *Tci*ALDO-1 cDNA was amplified from this cDNA in a PCR containing the oligonucleotide primers *Tci* aldo_FL-F1 (5'-CACCATGGCTTCCTACTCGCAGTA-3') and *Tci* aldo_FL-R1 (5'-TCAATAGGCATGATTAGCCAC-3'). The full-length gene was then transformed into TOP10 cells, and subsequently cloned into the expression vector

Champion pET100 Directional TOPO (ThermoFisher Scientific, Waltham, MA, USA), and transformed into *E. coli* One shot BL21 (DE3), according to the manufacturer's instruction. The construction integrity was checked by sequencing.

E. coli strain BL21 (DE3) transformed with pET 100 (as described by Umair et al., 2013b) using a NH₂ tag *Tci*ALDO-1 was grown in 10 mL Luria broth (LB) supplemented with 100 µg/mL ampicillin for 16 h at 30 °C and 250 rpm. The culture was diluted in LB with 100 µg/mL ampicillin and 1% glucose and grown to OD₆₀₀ of 0.6–0.8 at 30 °C and 250 rpm. Isopropyl-1-thio-β-D-galactopyranoside (IPTG) was added to a final concentration of 1 mM as described, and the culture grown at 30 °C and 250 rpm for an additional 16 h. Bacteria were harvested by centrifugation, as described before [23], and the soluble extract was obtained using enzymatic lysis and centrifugation.

2.4. Purification and Gel Electrophoresis

Recombinant *Tci*ALDO-1 was produced as recombinant poly-histidine protein, and was obtained by FPLC under native conditions using a Ni-NTA column (Qiagen, Germantown, MD, USA), and a Biologic DUO-FLOW BIO-RAD chromatography system (Bio-Rad, Auckland, New Zealand) as described before [24]. The protein was eluted using 500 mM imidazole, dialyzed overnight, and the concentration determined using the A280 nm assay with extinction coefficient (34,755 M⁻¹cm⁻¹) and molecular weight (43.8 KDa).

SDS-PAGE was performed as described previously [25] using NuPAGE Novex 4–12% Bis-Tris gels.

2.5. Bioinformatics

Alignment of protein sequences was performed using the Muscle alignment option in Geneious Prime (Biomatters Ltd., Auckland, New Zealand) with the Blossum 62 similarity matrix used to determine similarity to *H. contortus* and other helminth aldolases. The predicted tetramer structure of *Tci*ALDO-1 was constructed using SWISS-MODEL, a fully automated protein structure homology-modelling server, with default parameters.

2.6. *Tci*ALDO-1 Activity (E.C. 4.2.1.11)

The enzyme activity of *Tci*ALDO-1 was measured at 30 °C in a coupled assay with reversible conversion of fructose 1,6-bisphosphate to glyceraldehyde 3-phosphate and dihydroxyacetone phosphate using a Sigma aldolase kit (Catalogue # MAK223, St. Louis, MO, USA). NADH production was measured colorimetrically at 450 nm. The final reaction mixture (100 µL) contained assay buffer, enzyme mix, enzyme developer, recombinant protein (50 µg), and the substrate. NADH standards and the blank were set up as described by the manufacturer.

(1) The optimum pH was determined (in three independent biological replicates) with a substrate concentration of 0.5 mM fructose 1,6-bisphosphate with a pH range of 6 to 9. Subsequent assays were carried out at pH 7.5.

(2) The apparent K_m for fructose 1,6-bisphosphate was determined (in three independent biological replicates) in reaction mixtures containing 0–5 mM fructose 1,6-bisphosphate.

(3) The effects of EDTA as potential activators/inhibitors on recombinant *Tci*ALDO-1 with substrate concentrations of 0.5 mM fructose 1,6-bisphosphate and 10 mM EDTA were measured.

2.7. ELISA

To test for the presence of antibodies in the blood and saliva that react with the recombinant enzyme, saliva and serum samples were taken from parasite-exposed and -naïve sheep, as described previously [25]. Briefly, the plates were coated with the recombinant protein, blocked, and incubated with serial dilutions of serum or saliva. Immunoglobulins were then detected with the respective antibody. After incubation the color was developed with 3,3',5,5'-Tetramethylbenzidine (TMB).

2.8. Protein Modelling and Structural Analysis of *Tci*ALDO-1

The structural model of *Tci*ALDO-1 was generated from the amino acid sequence as previously described by [24,25]. Due to the lack of a perfect homologues template in PDB, homology modelling of the *Tci*ALDO-1 protein sequence was not possible, and therefore we used the threading method to model the protein structure using I-TASSER server [26]. The selected model had a C-score of -0.11 , and a TM value of 0.70 ± 0.12 , where the TM-score represents a metric of the degree of similarity of the two protein structures that the model was based on [27]. In addition, the C-score is a confidence score that estimates the quality of the predicted models. The structural model with highest C-score was further validated using Procheck [28] and ProSA-web [29]. The substrate Binding domain was identified, and active site residues were deduced and pictured using PyMol.

2.9. Data Analysis

Replicate data are presented as mean \pm SEM. Graph Prism v5 was used to plot kinetic data and estimate K_m and V_{max} . The kinetic data were analyzed using the non-linear fit function of Graph Prism and the best fit was shown to be a one-site binding hyperbola.

3. Results

3.1. *Tci*ALDO-1 Gene Sequence

The full length *T. circumcincta* *Tci*ALDO-1 sequence, comprising 1095 bp, has been deposited in Genbank as Accession No KX452943. The predicted protein consisted of 365 amino acids, as shown in Figure 1. A multiple alignment, using Alignment Geneious Prime, of the protein sequences of *Tci*ALDO-1 with homologues from *H. contortus*, *C. elegans*, *Caenorhabditis briggsae*, *Ancylostoma ceylanicum*, *C. sinensis*, *E. granulosus*, *Necator americanus*, *S. japonicum*, *O. viverrini*, and *H. glycines* is shown in Figure 1. Substrate binding sites and conserved regions in other homologues were identified, and shown to be completely conserved in *Tci*ALDO-1.

```

1
|
TciALDO-1      ----MASYSQPPPKKEDELRSIANAIIVAPGKGI LAADSTGSMDDKMKIGIGTENTEEQR
Haemonchus contortus aldolase ----MASHSQYLTKQEDELRSIANAIIVAPGKGI LAADSTGSMDDKMKQNIIGTENTEEQR
Caenorhabditis elegans aldo-1 ----MASYSQFLTKAQEDELRSIANAIIVT PGRKGI LAADSTGSMDDRLNSIIGLENTEENR
Caenorhabditis elegans aldo-2 MATVGGAFKDSLTAQKDELRSIAIAKIVQD PGRKGI LAADSTGTIGKRLDAINLENNETNR
Caenorhabditis briggsae aldolase ----MASYSQYLTKAQEDELRSIANAI IAPGKGI LAADSTGSMERKRLTSIIGLENNEENR
Drosophila melanogaster aldolase MTTYFNYPKELQDELRSIAQKIIVAPGKGI LAADSTGSMERKRLQDIIGVENTEDNR
Ancylostoma ceylanicum aldolase ----MASYSQFLPKKEDELRSIANAIIVSAGKGI LAADSTGSMERKRLKSIIGLENTEENR
Clonorchis sinensis aldolase ----MSLPKYLQPEQEARLKAIAIQIVQ PGRKGI LAADSTGTIGNRFKIKIIGVENSEENR
Echinococcus granulosus aldolase ----MARFVPIYCAEKMKELRENSAIVAPGKGL LAADSTSTIGKRFAAINLENTEENR
Necator americanus aldolase ----MASYSQYLTKKEDELRSIANAIIVASGKGI LAADSTGSMERKRLKSIIGLENTEENR
Schistosoma japonicum aldolase ----MPRFPPYLTEAQEDDLRQAQAI CAPGKGI LAADSTATMGKRLQDIIGVENEENR
Opisthorchis viverrini aldolase MPAVMRPFTEYLPKGLKELRDIANAIVAPGKGI LAADSTVTLGKRLKAINVENSEENR
Heterodera glycines aldolase MAEVGNISYRPLSEKQNELRAIAQKILQ PGRKGI LAADSTSGIIGKRFDTIIGLENTENR

120
|
TciALDO-1      RKYRQLLFTASPEMSKHI SGVIMFHETFYQKDDGTRFVDALKKQGI IPIGKVDKGVVEM
Haemonchus contortus aldolase RKYRQLLFTASPEMSKHI SGVIMFHETFYQKDDGTRFVDALKKQGI IPIGKVDKGVVEM
Caenorhabditis elegans aldo-1 RKYRQLLFTAGADLNKYI SGVIMFHETFYQKDDGKPTALLQEQGI IPIGKVDKGVVEM
Caenorhabditis elegans aldo-2 QKYRQLLFTT-PNLNQHISGVILYEETFHQSTDRGKFTDLLIKQGI IVPGIKLDLGVVPL
Caenorhabditis briggsae aldolase RKYRQLLFTAGADLNKYI SGVIMFHETFYQKDDGKPTALLQEQGI IPIGKVDKGVVPL
Drosophila melanogaster aldolase RAYRQLLFTSDPKLAENISGVILFHETLYQKADDDGTFPAEILKKKGI ILLGIKVDKGVVPL
Ancylostoma ceylanicum aldolase RKYRQLLFTGNPDLGKHI SGVIMFHETFYQKADDDGTRFVDALKKQGI IPIGKVDKGVVEM
Clonorchis sinensis aldolase RHYRQLLFTTDPCLANSI SGVILFHETFYQVADGVRVLDHLKRRKGI IPIGKLDKGVVPL
Echinococcus granulosus aldolase RAYRELLFTTDPPEFAKHI SGVILFHETFYQKTDGKRFVLLERGRVVPGIKVDLGVVPL
Necator americanus aldolase RKYRQLLFTGNPDLGKHI SGVIMFHETFYQKADDDGTRFVDVLLKKQGI IPIGKVDKGVVEM
Schistosoma japonicum aldolase RLYRQLLFSADHKLAQNI SGVILFEETLHQKSDGKTLPTLLAERHI IPIGKVDKGVVPL
Opisthorchis viverrini aldolase RAYRQLLFSADPVLARNI SGVILYHETLYQKTDGGMPLVRLLDQRGI IPIGKVDKGVVPL
Heterodera glycines aldolase RRYRQLLFTT-PSFGNLSGVILFDETFRQSTDNQVRFVDVIKAGAVAGIKVDTGVVPL

```

Figure 1. Cont.

		180
TciALDO-1	AGTVGEGTTQGMDDLNRCAQYKKGDAQFAKWRVCVHKISATTPSHMALVEIAEVLARYAS	
Haemonchus contortus aldolase	AGTVGEGTTQGMDDLNRCAQYKKGDAQFAKWRVCVHKISATTPSHMALVEIAEVLARYAS	
Caenorhabditis elegans aldo-1	AGTIGEGTTQGLDDLNRCAQYKKGDAQFAKWRVCVHKISSTTPSVTALKEIASNLARYAS	
Caenorhabditis elegans aldo-2	AGTIGEGTTQGLDLAERAAAFKGGGQFAKWRVCVHKISSTTPSHLGMLENANVRLARYAS	
Caenorhabditis briggsae aldolase	AGTIGEGTTQGLDDLNRCAQYKKGDAQFAKWRVCVHKISSTTPSVTALKEVAQVRLARYAS	
Drosophila melanogaster aldolase	FGSEDEVTTQGLDDLNRCAQYKKGDCDFAKWRVCVHKISSTTPSYQSIENANVRLARYAS	
Ancylostoma ceylanicum aldolase	AGTVGEATTQGLDDLNRCAQYKKGDAQFAKWRVCVHKISSTTPSHALVEIAQVRLARYAS	
Clonorchis sinensis aldolase	AGTLNECTTQGLDGLAERCAQYKKGDAQFAKWRVCVHKISSTTPSYLAMMENANVRLARYAS	
Echinococcus granulosus aldolase	GGTADDECTQGLDNLQRCAQYKKGDCRFKWRVCVHKISSTHNPVSYLAMLENANVRLARYAS	
Necator americanus aldolase	AGTVGEATTQGLDDLNRCAQYKKGDAQFAKWRVCVHKISVTTTPSHALVEIAQVRLARYAS	
Schistosoma japonicum aldolase	AGTDNETTTQGLDDLNRCAEYKRLGCRFAKWRVCVHKISSTHNPVSYQSIENANVRLARYAS	
Opisthorchis viverrini aldolase	PGTPEECTTQGLDGLSDRCAQYKKGDCDFAKWRVCVHKISDRTTPSYLAMKENANVRLARYAS	
Heterodera glycines aldolase	AGTLDEGTTQGLDKLSDRCAEYKKGDCDFAKWRVCVHKISGAKHPSHLAMMENANVRLARYAS	
		240
TciALDO-1	ICQONGLVPIVEPEEILPDGEHDIRCRKITETVLSYCYRALNDHHVYLEGTLTKPNMVT	
Haemonchus contortus aldolase	ICQONGLVPIVEPEEILPDGEHDIRCRKITETVLSYCYRALNDHHVYLEGTLTKPNMVT	
Caenorhabditis elegans aldo-1	ICQONGLVPIVEPEEILPDGEHCLARQKITEVTVLSYVYHALNEHHVYLEGTLTKPNMVT	
Caenorhabditis elegans aldo-2	ICQONGLVPIVEPEEILPDGEHDLARQKITEVTVLSYVYKALADHHVYLEGTLTKPNMVT	
Caenorhabditis briggsae aldolase	ICQONGLVPIVEPEEILPDGEHDLARQKITEVTVLSYVYHALNEHHVYLEGTLTKPNMVT	
Drosophila melanogaster aldolase	ICQSRIVPIVEPEEILPDGDHDLRAQKITEVTVLAAVYKALSDHHVYLEGTLTKPNMVT	
Ancylostoma ceylanicum aldolase	ICQONGLVPIVEPEEILPDGEHDIRCRKITETVLSYCYRALNDHHVYLEGTLTKPNMVT	
Clonorchis sinensis aldolase	ICQONGLVPIVEPEEILPDGDHDLARQKITEVTVLSYCYRALNDHHVYLEGTLTKPNMVT	
Echinococcus granulosus aldolase	ICQONGLVPIVEPEEILPDGDHDLARQKITEVTVLSYCYRALNDHHVYLEGTLTKPNMVT	
Necator americanus aldolase	ICQONGLVPIVEPEEILPDGEHDIRCRKITETVLSYCYRALNDHHVYLEGTLTKPNMVT	
Schistosoma japonicum aldolase	ICQONGLVPIVEPEEILPDGDHDLARQKITEVTVLSYCYRALNDHHVYLEGTLTKPNMVT	
Opisthorchis viverrini aldolase	ICQONGLVPIVEPEEILPDGDHDLARQKITEVTVLSYCYRALNDHHVYLEGTLTKPNMVT	
Heterodera glycines aldolase	ICQONGLVPIVEPEEILPDGDHDLARQKITEVTVLSYCYRALNDHHVYLEGTLTKPNMVT	
		300
TciALDO-1	GQAFKGGKPSHDEIALATITLQRVSPAAPVGVVFLSGGQSEEDATLNLNAMNKLDTKKP	
Haemonchus contortus aldolase	GQAFKGGKPSHDEIALATITLQRVSPAAPVGVVFLSGGQSEEDATLNLNAMNKLDTKKP	
Caenorhabditis elegans aldo-1	QGSFTGEKPSNADIGLATVTLQRVSPAAPVGVVFLSGGQSEEDATLNLNAMNKVGGKPK	
Caenorhabditis elegans aldo-2	QGS--SASKASHEAIGLATVTLRRGVSPAAPVGVVFLSGGQSEEDATLNLNAMNKVQLGKPK	
Caenorhabditis briggsae aldolase	QGSFTGEKPSNADIGLATVTLQRVSPAAPVGVVFLSGGQSEEDATLNLNAMNKVGGKPK	
Drosophila melanogaster aldolase	QGS--AKNTPPEEIALATVQALRRTVPAAVGVVFLSGGQSEEDATLNLNAMNKVQLRP	
Ancylostoma ceylanicum aldolase	QGSFKGGKPSDDVGGKATVTLQRVSPAAPVGVV-----AGRR	
Clonorchis sinensis aldolase	QGSCT--QRVTPPEEIGLATVTLQRVSPAAPVGVVFLSGGQSEEEAAILNSAINCVGHPK	
Echinococcus granulosus aldolase	QGSCT--KRYSYVDNARATVEALQRTVPAAPVGVVFLSGGQSEEDATLNLNAMNKVGGKPK	
Necator americanus aldolase	QGSFKGGKPSNADVGLATVTLQRVSPAAPVGVVFLSGGQSEEEAAILNLNAMNKVAGKRP	
Schistosoma japonicum aldolase	QGACK--KAYTPQENALATVRLQRVSPAAPVGVVFLSGGQSEEDATLNLNAMNKVGGKPK	
Opisthorchis viverrini aldolase	QGSHS--HKYSVEQNVAATVQALQRTVPAAPVGVVFLSGGQSEVEATQNLNAMNKVAGKRP	
Heterodera glycines aldolase	QGSHS--PKATPDQIGLATVTLRRSVPIAVGVVFLSGGQSEIEATLNLNAMNKVGGKPK	
		360
TciALDO-1	WALTFSYGRALQASCMKWKGGKDNVVKDAQVFMQRAQANSALALGKYSGDPNADKAASQ	
Haemonchus contortus aldolase	WALTFSYGRALQASAMAKWKGKDNVPAKAVFMQRAQANSALALGKYSGDPNADKAASQ	
Caenorhabditis elegans aldo-1	WALTFSYGRALQASCLAKWAGKDNIAAAQEVLLHRAQVNSLASVGGKYGDSADAAASQ	
Caenorhabditis elegans aldo-2	WALTFSYGRALQASVLAQWGGKDNIAAAQKTLHRSKANGDASLGKYAGEDAA--GAAE	
Caenorhabditis briggsae aldolase	WALTFSYGRALQASCLAKWAGKDNIAAAQEVLLHRAQVNSLASVGGKYGDSADAAASQ	
Drosophila melanogaster aldolase	WALTFSYGRALQASVLRWAGKDNIAAAQEVLLHRAQVNSLASVGGKYGDSADAAASQ	
Ancylostoma ceylanicum aldolase	WVLTFSYGRALQASTLAKWAGKDNIAAAQEVLLHRAQVNSLASVGGKYGDSADAAASQ	
Clonorchis sinensis aldolase	WVLTFSYGRALQASVLAQWGGKDNIAAAQEVLLHRAQVNSLASVGGKYGDSADAAASQ	
Echinococcus granulosus aldolase	WVLTFSYGRALQASVLAQWGGKDNIAAAQEVLLHRAQVNSLASVGGKYGDSADAAASQ	
Necator americanus aldolase	WVLTFSYGRALQASCLAKWAGKDNIAAAQEVLLHRAQVNSLASVGGKYGDSADAAASQ	
Schistosoma japonicum aldolase	WALTFSYGRALQASVLAQWGGKDNIAAAQEVLLHRAQVNSLASVGGKYGDSADAAASQ	
Opisthorchis viverrini aldolase	WALTFSYGRALQASVLAQWGGKDNIAAAQEVLLHRAQVNSLASVGGKYGDSADAAASQ	
Heterodera glycines aldolase	WVLTFSYGRALQASVLAQWGGKDNIAAAQEVLLHRAQVNSLASVGGKYGDSADAAASQ	
	Identity (%)	
TciALDO-1	SFLVANHAY	
Haemonchus contortus aldolase	SFLVANHAY 94	
Caenorhabditis elegans aldo-1	SFLVANHSY 78	
Caenorhabditis elegans aldo-2	SFLVAKHSY 61	
Caenorhabditis briggsae aldolase	SFLVANHAY 77	
Drosophila melanogaster aldolase	SFLVANHAY 79	
Ancylostoma ceylanicum aldolase	SFLVANHAY 65	
Clonorchis sinensis aldolase	TLFVPSHAY 62	
Echinococcus granulosus aldolase	SFLVANHAY 64	
Necator americanus aldolase	SFLVANHAY 86	
Schistosoma japonicum aldolase	SFLVANHAY 62	
Opisthorchis viverrini aldolase	SFLSANHAY 63	
Heterodera glycines aldolase	SFLVAKHAY 63	

Figure 1. Multiple sequence alignment of aldolases from *Teladorsagia circumcincta* (GI: KX452943), *Haemonchus contortus* (GI: ADT61995), *Caenorhabditis elegans* aldo-1 (GI: CAB03291), *Caenorhabditis elegans* aldo-2 (GI: CCD65997), *Caenorhabditis briggsae* (GI: XP002643138), *Ancylostoma ceylanicum* (GI: EPB73313), *Clonorchis sinensis* (GI: GAA50927), *Echinococcus granulosus* (GI: EUB64508), *Necator americanus* (GI: XP013291330), *Schistosoma japonicum* (GI: CAX78614), *Opisthorchis viverrini* (GI: OON18662), and *Heterodera glycines* (GI: AAG47838), homologues. Amino acid residues indicated in the marked box are essential to the aldolase activity.

To identify the active site as well as infer both functional and structural characteristics, the 3D model of *Tci*ALDO-1 was modelled via the threading method using the I-TASSER server (Figure 2). Initially five models were generated for *Tci*ALDO using ten different templates, and reported by ten different threading programs [30], to provide coverage of the different structural parts of the query sequence. The C-score of the best five models were less than -2.9 , the expected TM Score was <0.7 , and the normalized z-scores were less than 7.93. The I-TASSER modelled protein produced was similar to the parent molecule, with a C-score of -0.11 and a TM value of 0.70, and all within acceptable ranges. A detailed description of the selected 3D structural model of *Tci*ALDO and different domains is depicted in Figure 2. Moreover, the superimposed best structural model was found to correspond to the monomer of 3TU9 [31] as well as the 1,6-fructose diphosphate ligand (2FP) binding site, and catalytic and active site residues that fall within 4 \AA of the substrate (Ala-68, Ser-75, Ser-72, Glu-71, Asp-70, Lys-144, Lys-183, Arg-185, Glu-224, Lys-266, Leu-308, Gly-310, Ser-309, Tyr-339, Arg-341, and Gly-340). It is noteworthy that the lysine at position 230 is the residue where Schiff base intermediates are formed.

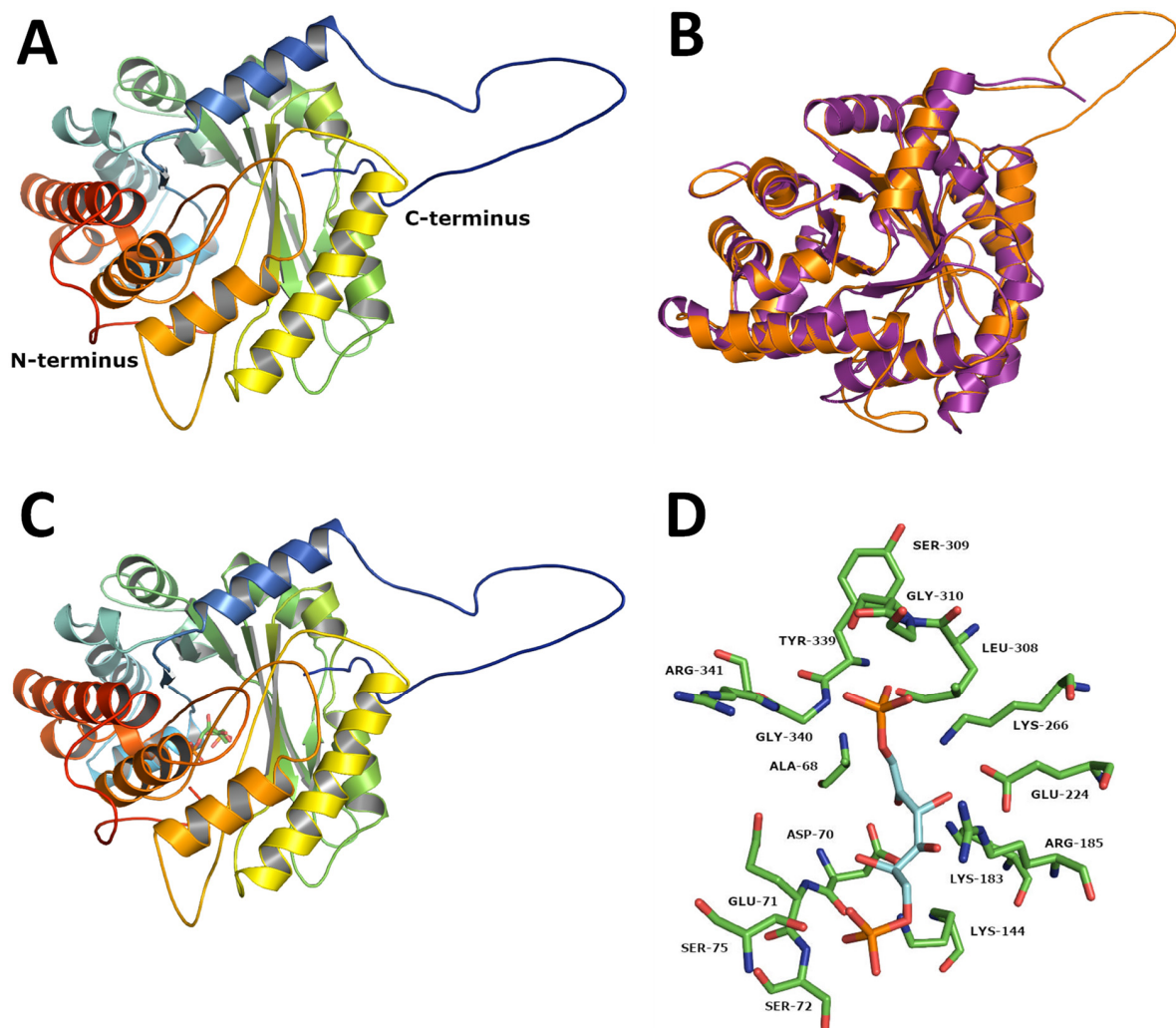


Figure 2. The predicted tertiary structure of *Tci*ALDO-1. (A) The predicted tertiary structure of *Tci*ALDO-1 monomer. (B) Superposition of the predicted tertiary structure of *Tci*ALDO-1 from *T. circumcincta* (orange) and 3TU9 (purple). 3TU9 is the repository code for the coordinates of rabbit muscle aldolase stored at the protein data bank (<https://www.rcsb.org/structure/3TU9>), and was the template for our model. (C) Location of the active site within *Tci*ALDO-1. (D) The active site of *Tci*ALDO-1 (in green) within 4 \AA of the superimposed 2FP (in blue). 2FP is an abbreviation for “1,6-fructose diphosphate”, also stored at the protein data bank (<https://www.rcsb.org/ligand/2FP>), and was the ligand modelled for our structure.

3.2. Recombinant Protein Expression

A number of varying conditions were used in the trial expression, and based on which, maximal production of functional recombinant ALDO-1 was obtained in the *E. coli* strain BL21 (DE3) when expression was induced with 1 mM IPTG at 30 °C for 16 h. The purified N-terminal His recombinant *Tci*ALDO-1 protein appeared as a single band of about 44 kDa (Figure 3).

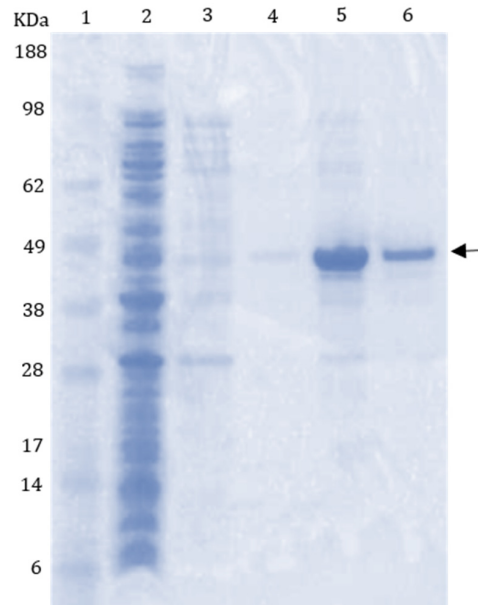


Figure 3. SDS-PAGE of recombinant *Tci*ALDO-1. Lane 1: standards; lane 2: unbound; lane 3: wash 1; lane 4: wash 2; lane 5: elution 1; lane 6: elution 2; lane 7: standards. The arrow indicates recombinant purified *Tci*ALDO-1.

3.3. Enzyme Assays

The optimum pH for recombinant *Tci*ALDO-1 activity at 30 °C was 7.5 (Figure 4). The apparent K_m for fructose 1,6-bisphosphate was $0.24 \pm 0.01 \mu\text{M}$ and the V_{max} was $432 \text{ nmol min}^{-1} \text{ mg}^{-1} \text{ protein}$ (mean \pm SEM, $n = 3$) (Figure 5). The kinetic data best fit a one-site binding hyperbola with a Hill Coefficient of 1.70.

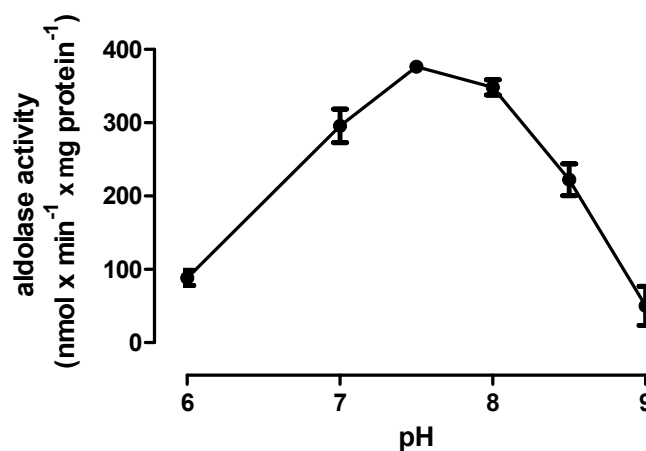


Figure 4. Effects of pH on the activity of recombinant *Tci*ALDO-1 at 30 °C (mean \pm SEM, $n = 3$, independent biological replicates). Enzyme activity was estimated from the rate of NADH production, which was measured colorimetrically at 450 nm.

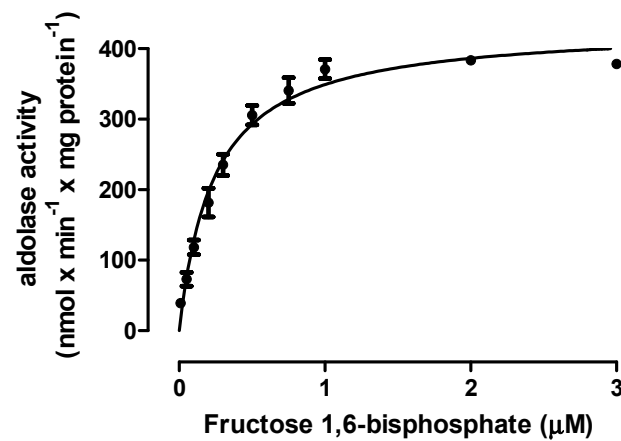


Figure 5. Effects of varying substrate concentration on the activity of recombinant *TciALDO-1* at 30 °C (mean \pm SEM, $n = 3$, independent biological replicates). Enzyme activity was estimated from the rate of NADH production, which was measured colorimetrically at 450 nm.

3.4. Host Recognition

Recombinant *TciALDO-1* was recognized in an ELISA by antibodies in both serum and saliva collected from immune sheep exposed to nematodes in the field (Figure 6). There was no antibody detection when serum or saliva samples from parasite-naïve animals was used.

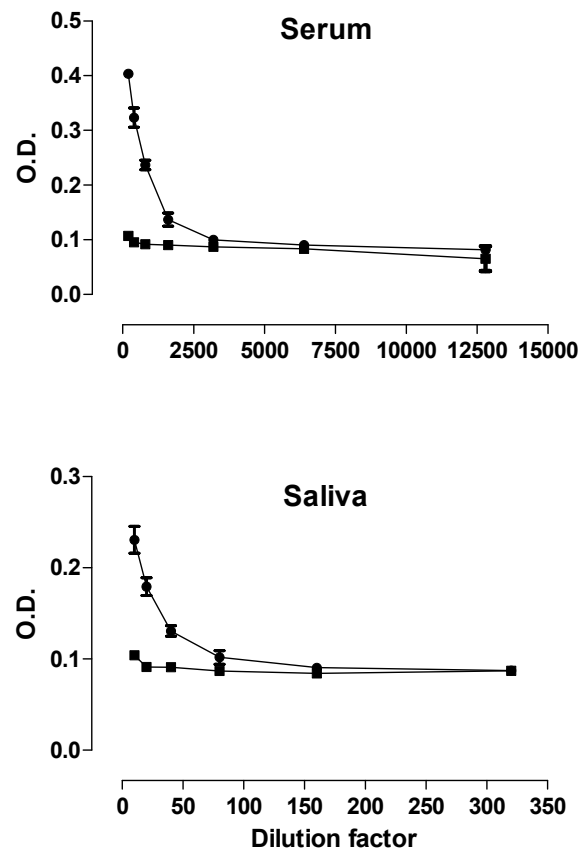


Figure 6. Recognition of *TciALDO-1* by serially diluted serum (IgG) (top) or saliva (IgA) (bottom) (●) from parasite-exposed animals, but not by serum or saliva (■) from parasite-naïve animals. Pooled serum or saliva samples were used in the assays, the assays were performed three times, and the data presented as SEM.

4. Discussion

To the best to our knowledge, this is the first report of a 1095 bp full length cDNA sequence encoding *T. circumcincta* aldolase (*Tci*ALDO-1) amplified from adult *T. circumcincta* cDNA, cloned and expressed in *E. coli*. The 365 amino acid *Tci*ALDO-1 protein expressed in *E. coli* was typical of aldolase monomers of many species, and had 77–94% similarity to the aldolase of other nematodes, and 62–64% similarity to that of cestodes and trematodes (Figure 1).

The 3D-structure, as well as binding and catalytic sites have been determined for a wide range of FBAs, and are known to be highly conserved (Figure 2) [2,32,33]. This was also true for other helminth homologues (Figure 1), although there were minor differences in the trematode and cestode aldolase sequences, in which serine was replaced by threonine at amino acid 38. The importance of structurally characterizing the aldolase protein has been shown by its differential expression involved in in-vitro molting and/or exsheathment in other economically important gastrointestinal parasites [34]. Overall, the validation statistics and features structure imply that there is a need for further characterization of the structure, possibly with future efforts aimed at generating a crystal structure of *Tci*ALDO.

The kinetic properties of the recombinant *Tci*ALDO-1 were generally similar to those of enzymes of other species. The optimum pH for *Tci*ALDO-1 activity at 30 °C was pH 7.5 (Figure 4), similar to that for the aldolase of *H. contortus* [6]. The enzyme was very active at 30 °C (V_{\max} 432 ± 23 nmoles.min⁻¹.mg protein⁻¹) and of a similar magnitude to activities at 40–45 °C of the closely related aldolases of *H. contortus* [6] and *C. sinensis* [10]. *Tci*ALDO-1 activity was unchanged by the addition of 10 mM EDTA, indicating that the enzyme was a class I and not class II aldolase, which is strongly inhibited by EDTA [2]. The apparent K_m of *Tci*ALDO-1 for the substrate fructose 1,6-bisphosphate was 0.2 ± 0.01 µM (Figure 5). This is higher than the 0.06 µM reported for recombinant *S. japonicum* aldolase [11], but lower than the very variable values reported for the partially purified *Ascaris suum* [35] or *H. contortus* aldolases [36]. Kinetic properties may be more accurately reflected by recombinant enzymes than purified proteins, and this suggest that parasitic helminths may have more active enzymes than their hosts [13].

Recombinant *Tci*ALDO-1 was antigenic, and antibodies in both serum and saliva from field-immune, but not nematode-naïve, sheep recognized recombinant *Tci*ALDO-1 in an ELISA (Figure 6). Aldolase, like many other glycolytic enzymes, has both intra- and extra-cellular activities in pathogens, in addition to its enzymatic function [16], which have been suggested to facilitate their establishment in the host. These appear to be essential to the successful establishment of many pathogens, including helminths. This is supported by the protection against infection induced by vaccination of mice with the aldolase of *S. mansoni* [18], or fish with the aldolase of several pathogenic bacteria [37].

5. Conclusions

A 1095 bp full length cDNA encoding *Tci*ALDO-1 was cloned and expressed in *E. coli*. The protein sequence showed high levels of homology with other helminth aldolases and all the active and substrate binding sites were completely conserved. Enzyme assays were performed using the recombinant protein showed biochemical properties of *Tci*ALDO-1 were generally similar to those of enzymes of other species. Serum and saliva from the sheep immune to the parasite infection recognized recombinant *Tci*ALDO-1. With significant differences in the structure from the mammalian aldolases and with a critical role in the metabolism, recombinant *Tci*ALDO-1 has a potential as a vaccine candidate to control the parasite infection.

Author Contributions: Conceptualization, S.U.; Formal analysis, S.U. and N.P.; Funding acquisition, S.U.; Investigation, C.B.; Methodology, C.B.; Project administration, S.U.; Supervision, S.U. and H.S.; Writing—original draft, S.U. and H.S.; Writing—review & editing, S.U., and H.S. All authors have read and agreed to the published version of the manuscript.

Funding: The financial support of AGMARDT (Grant No. P14003) is thankfully acknowledged.

Institutional Review Board Statement: Use of lambs for parasite culturing and harvesting adult worms for molecular biology studies was approved in protocol #13502 by the AgResearch Grasslands Animal Ethics Committee (2 August 2014).

Informed Consent Statement: Not applicable.

Data Availability Statement: The raw data can be made available on request.

Acknowledgments: The authors would like to thank Axel Heiser and Sandeep Gupta for critically reviewing the manuscript.

Conflicts of Interest: The authors declare no conflict of interest.

References

1. Marsh, K.; Lebherz, H.G. Fructose-bisphosphate aldolases; an evolutionary history. *Trends Biochem. Sci.* **1992**, *17*, 110–118. [[CrossRef](#)]
2. Gefflaut, T.; Blonski, C.; Perie, J.; Willson, M. Class I aldolases: Substrate specificity, mechanism, inhibitors and structural aspects. *Prog. Biophys. Mol. Biol.* **1995**, *63*, 301–340. [[CrossRef](#)]
3. Sánchez, L.B.; Horner, D.S.; Moore, D.V.; Henze, K.; Embley, T.; Müller, M. Fructose-1,6-bisphosphate aldolases in amitochondriate protists constitute a single protein subfamily with eubacterial relationships. *Gene* **2002**, *295*, 51–59. [[CrossRef](#)]
4. Tittmann, K. Sweet siblings with different faces: The mechanisms of FBP and F6P aldolase, transaldolase, transketolase and phosphoketolase revisited in light of recent structural data. *Bioorg. Chem.* **2014**, *57*, 263–280. [[CrossRef](#)] [[PubMed](#)]
5. Inoue, T.; Yatsuki, H.; Kusakabe, T.; Joh, K.; Takasaki, Y.; Nikoh, N.; Miyata, T.; Hori, K. *Caenorhabditis elegans* has two isozymic forms, CE-1 and CE-2, of fructose-1,6-bisphosphate aldolase which are encoded by different genes. *Arch. Biochem. Biophys.* **1997**, *339*, 226–234. [[CrossRef](#)] [[PubMed](#)]
6. Yan, R.; Xu, L.; Wang, J.; Song, X.; Li, X. Cloning and characterization of aldolase from parasitic nematode *Haemonchus contortus*. *J. Anim. Vet. Adv.* **2013**, *12*, 478–486.
7. Kovaleva, E.S.; Masler, E.P.; Subbotin, S.A.; Chitwood, D.J. Molecular characterization of aldolase from *Heterodera glycines* and *Globodera rostochiensis*. *J. Nematol.* **2005**, *37*, 292–296.
8. El-Dabaa, E.; Mei, H.; El-Sayed, A.; Karim, A.M.; Eldesoky, H.M.; Fahim, F.A.; LoVerde, P.T.; Saber, M.A. Cloning and characterization of *Schistosoma mansoni* fructose-1,6-bisphosphate aldolase isoenzyme. *J. Parasitol.* **1998**, *84*, 954–960. [[CrossRef](#)] [[PubMed](#)]
9. Lorenzatto, K.R.; Monteiro, K.M.; Paredes, R.; Paludo, G.P.; da Fonsêca, M.M.; Galanti, N.; Zaha, A.; Ferreira, H.B. Fructose-bisphosphate aldolase and enolase from *Echinococcus granulosus*: Genes, expression patterns and protein interactions of two potential moonlighting proteins. *Gene* **2012**, *506*, 76–84. [[CrossRef](#)]
10. Li, S.; Bian, M.; Wang, X.; Chen, X.; Xie, Z.; Sun, H.; Jia, F.; Liang, P.; Zhou, C.; He, L.; et al. Molecular and biochemical characterizations of three fructose-1,6-bisphosphate aldolases from *Clonorchis sinensis*. *Mol. Biochem. Parasitol.* **2014**, *194*, 36–43. [[CrossRef](#)]
11. Hu, Q.; Xie, H.; Zhu, S.; Liao, D.; Zhan, T.; Liu, D. Cloning, expression and partial characterization of FBPA from *Schistosoma japonicum*, a molecule on that the fluke may develop nutrition competition and immune evasion from human. *Parasitol. Res.* **2015**, *114*, 3459–3468. [[CrossRef](#)] [[PubMed](#)]
12. Prompipak, J.; Senawong, T.; Jokchaiyaphum, K.; Siriwes, K.; Nuchadomrong, S.; Laha, T.; Sripa, B.; Senawong, G. Characterization and localization of *Opisthorchis viverrini* fructose-1,6-bisphosphate aldolase. *Parasitol. Int.* **2017**, *66*, 413–418. [[CrossRef](#)] [[PubMed](#)]
13. Reznick, A.Z.; Gershon, D. Purification of fructose-1,6-diphosphate aldolase from the free-living nematode *Turbatrix aceti*. Comparison of properties with those of other class I aldolases. *Int. J. Biochem.* **1977**, *8*, 53–59. [[CrossRef](#)]
14. Reznick, A.Z.; Gershon, D. Age related alterations in purified fructose-1,6-diphosphate aldolase from the nematode *Turbatrix aceti*. *Mech. Aging Dev.* **1977**, *6*, 53–59. [[CrossRef](#)]
15. Zeelon, P.; Gershon, H.; Gershon, D. Inactive enzyme molecules in aging organisms. Nematode fructose 1,6-diphosphate aldolase. *Biochemistry* **1973**, *12*, 1743–1750. [[CrossRef](#)]
16. Gómez-Arreaza, A.; Acosta, H.; Quiñones, W.; Concepción, J.L.; Michels, P.A.; Avilán, L. Extracellular functions of glycolytic enzymes of parasites: Unpredicted use of ancient proteins. *Mol. Biochem. Parasitol.* **2014**, *193*, 75–81. [[CrossRef](#)]
17. Ramajo-Hernández, A.; Sánchez, R.P.; Martín, V.R.; Oleaga, A. *Schistosoma bovis*: Plasminogen binding in adults and the identification of plasminogen-binding proteins from the worm tegument. *Exp. Parasitol.* **2007**, *115*, 83–91.
18. Marques, H.H.; Zouain, C.S.; Torres, C.B.B.; Oliveira, J.S.; Alves, J.B.; Goes, A.M. Protective effect and granuloma down-modulation promoted by RP44 antigen a fructose 1,6-bisphosphate aldolase of *Schistosoma mansoni*. *Immunobiology* **2008**, *213*, 437–446. [[CrossRef](#)]
19. Guillou, F.; Roger, E.; Moné, Y.; Rognon, A.; Grunau, C.; Théron, A.; Mitta, G.; Coustau, C.; Gourbal, B.E. Excretory–secretory proteome of larval *Schistosoma mansoni* and *Echinostoma caproni*, two parasites of *Biomphalaria glabrata*. *Mol. Biochem. Parasitol.* **2007**, *155*, 45–56. [[CrossRef](#)]

20. Morassutti, A.L.; Levert, K.; Pinto, P.M.; da Silva, A.J.; Wilkins, P.; Graeff-Teixeira, C. Characterization of *Angiostrongylus cantonensis* excretory–secretory proteins as potential diagnostic targets. *Exp. Parasitol.* **2012**, *130*, 26–31. [[CrossRef](#)]
21. Umair, S.; Ria, C.; Knight, J.S.; Simpson, H.V. Sarcosine metabolism in *Haemonchus contortus* and *Teladorsagia circumcincta*. *Exp. Parasitol.* **2013**, *134*, 1–6. [[CrossRef](#)] [[PubMed](#)]
22. Umair, S.; Bouchet, C.L.G.; Knight, J.S.; Pernthaner, A.; Simpson, H.V. Molecular and biochemical characterisation and recognition by the immune host of the glyceraldehyde 3-phosphate dehydrogenase (GAPDH) of the abomasal nematode parasite *Teladorsagia circumcincta*. *Exp. Parasitol.* **2017**, *181*, 40–46. [[CrossRef](#)] [[PubMed](#)]
23. Umair, S.; Bouchet, C.L.G.; Knight, J.S.; Pernthaner, A.; Simpson, H.V. Molecular and biochemical characterisation and recognition by the immune host of the enolase of the abomasal nematode parasite *Teladorsagia circumcincta*. *Exp. Parasitol.* **2017**, *172*, 30–38. [[CrossRef](#)] [[PubMed](#)]
24. Umair, S.; Bouchet, C.L.G.; Deng, Q.; Palevich, N.; Simpson, H.V. Characterisation of a *Teladorsagia circumcincta* glutathione transferase. *Mol. Biochem. Parasitol.* **2020**, *239*, 111316. [[PubMed](#)]
25. Umair, S.; Bouchet, C.; Palevich, N.; Simpson, H.V. Characterisation and structural analysis of glyoxylate cycle enzymes of *Teladorsagia circumcincta*. *Mol. Biochem. Parasitol.* **2020**, *240*, 111335. [[CrossRef](#)] [[PubMed](#)]
26. Yang, J.; Yan, R.; Roy, A.; Xu, D.; Poisson, J.; Zhang, Y. The I-TASSER Suite: Protein structure and function prediction. *Nat. Methods* **2015**, *12*, 7–8. [[CrossRef](#)] [[PubMed](#)]
27. Zhang, Y.; Skolnick, J. Scoring function for automated assessment of protein structure template quality. *Proteins* **2004**, *57*, 702–710. [[CrossRef](#)]
28. Laskowski, R.A.; Rullmann, J.A.C.; MacArthur, M.W.; Kaptein, R.; Thornton, J.M. AQUA and PROCHECK-NMR: Programs for checking the quality of protein structures solved by NMR. *J. Biomol. NMR* **1996**, *8*, 477–486. [[CrossRef](#)]
29. Wiederstein, M.; Sippl, M.J. ProSA-web: Interactive web service for the recognition of errors in three-dimensional structures of proteins. *Nucleic Acids Res.* **2007**, *35*, W407–W410. [[CrossRef](#)]
30. Essmann, U.; Perera, L.; Berkowitz, M.L.; Darden, T.; Lee, H.; Pedersen, L.G. A smooth particle mesh Ewald method. *J. Chem. Phys.* **1995**, *103*, 8577–8593. [[CrossRef](#)]
31. Mabilia-Bassiloua, C.G.; Arthus-Cartier, G.; Hannaert, V.; Thérisod, H.; Sygusch, J.; Thérisod, M. Mannitol bis-phosphate based inhibitors of fructose 1,6-bisphosphate aldolases. *ACS Med. Chem. Lett.* **2011**, *2*, 804–808. [[CrossRef](#)] [[PubMed](#)]
32. Dalby, A.; Dauter, Z.; Littlechild, J.A. Crystal structure of human muscle aldolase complexed with fructose-1,6-bisphosphate: Mechanistic implications. *Protein Sci.* **1999**, *8*, 291–297. [[CrossRef](#)] [[PubMed](#)]
33. Roslan, H.A.; Hossain, M.A.; Gerunsin, J. Molecular and 3D-structural characterization of fructose-1,6-bisphosphate aldolase derived from *Metroxlon sagu*. *Braz. Arch. Biol. Technol.* **2017**, *60*, 1–21. [[CrossRef](#)]
34. Ondrovics, M.; Gasser, R.B.; Joachim, A. Recent Advances in Elucidating Nematode Moulting—Prospects of Using *Oesophagostomum dentatum* as a model. *Adv. Parasitol.* **2016**, *91*, 233–264. [[PubMed](#)]
35. Kochman, M.; Kwiatkowska, D. Purification and properties of fructose diphosphate aldolase from *Ascaris suum* muscle. *Arch. Biochem. Biophys.* **1972**, *152*, 856–868. [[CrossRef](#)]
36. Rhodes, M.B. *Haemonchus contortus*: Enzymes. II. Fructose diphosphate aldolase. *Exp. Parasitol.* **1972**, *31*, 332–340. [[CrossRef](#)]
37. Sun, Z.; Shen, B.; Wu, H.; Zhou, X.; Wang, Q.; Xiao, J.; Zhang, Y. The secreted fructose-1,6-bisphosphate aldolase as a broad-spectrum vaccine candidate against pathogenic bacteria in aquaculture. *Fish Shellfish Immunol.* **2015**, *46*, 638–647. [[CrossRef](#)]